AIAA JOURNAL
Vol. 38, No. 12, December 2000

Adaptive QUICK-Based Scheme to Approximate Convective Transport

K. B. Kuan* and C. A. Lin†
National Tsing Hua University, Hsinchu 30013, Taiwan, Republic of China

A new adaptive high-order-accurate convection scheme that satisfies the unsteady total variation diminishing principle has been developed. The second-order accuracy of the proposed scheme was verified by numerical experiments on the unsteady linear and nonlinear scalar equations. The new scheme was further applied to one-dimensional unsteady compressible shock tube and steady nozzle flows and a two-dimensional shock reflection problem. Predicted results indicate that the present method returns a high order of accuracy and oscillation free results.

I. Introduction

THE desirable features of schemes to approximate convective transport are of high-order accuracy, stability, boundedness, and algorithmic simplicity. These can be easily satisfied for problems with smoothly varying dependent variables. However, in turbulent flows or compressible flows in the presence of shock, the appearance of sharp gradients of the transported variables makes the approximation of the convection term a difficult task.

A bounded solution is crucial on physical grounds. For example, the mixture fraction of reacting flows and the normal components of the Reynolds stresses cannot fall below zero. To obtain stable and bounded solutions, a first-order upwind-difference scheme is often adopted; however, this scheme (with a leading second-order truncation error resembling a viscous process) is highly diffusive in situations where the flow direction is oblique or skewed relative to the numerical grid. To remedy this, higher-order schemes are usually preferred due to their lack of numerical dissipation; however they also inevitably generate oscillations when excited by features such as a shock or steep variations of the transported properties.

There are several approaches to counteract the oscillations. For example, it is possible to obtain bounded solutions by adding additional artificial viscosity to the finite difference schemes. Therefore, one plausible approach is to add explicitly artificial diffusion flux[1] to the convection term, which is in general approximated by central differencing. These dissipation terms, however, usually contain problem-dependent parameters, which must be tuned in advance. Another approach is the adoption of higher-order upwinding schemes. The high-order upwind convection scheme, QUICK,[2] for example, though handling well convective transport for problems with smoothly varying dependent variables, introduces unphysical overshoots and oscillatory results in regions where the convected variables experience sharp changes in gradients (or discontinuities) under highly convective conditions. Because this scheme is widely used to compute turbulent flows within the pressure correction and the segregated approach, a number of schemes, for example SHARP[3] and SMART,[4] have been proposed to overcome this defect; however, these schemes, though performing well in passive scalar problems, are not bounded in situations such as shock tube flows.[5,6]

Total variation diminishing (TVD) schemes[7–10] possess several attractive features, such as delivering well-resolved, nonoscillatory discontinuities and convergent solutions. It is possible to derive methods with a high order of accuracy, that are TVD. To remedy the unbounded solution of the QUICK scheme, bounded-QUICK schemes,[6,11] which are based on the TVD constraints proposed by Sweby,[9] were proposed.

However, Sweby's TVD constraints were shown to represent much more restrictive conditions than the constraints accounting for the Courant number effect.[12–15] In the present study, a new high-order-accurate convection scheme that is based on the QUICK scheme and satisfies the unsteady TVD principle will be presented. The new scheme is to be applied to pure convection problems and compressible flows with discontinuity of the transported variables. The merits of the adoption of the unsteady TVD constraints will also be addressed.

II. Mathematical Formulation

Before proceeding to the derivation of the new scheme, it is essential to discuss the TVD principle. For simplicity, consider first a linear scalar equation:

$$\frac{\partial \phi}{\partial t} + a\frac{\partial \phi}{\partial x} = 0, \qquad a > 0 \tag{1}$$

According to Harten,[7] the principle of monotonicity properties dictates the solution of Eq. (1) as a function of time to have the following qualities. 1) No new local extrema may be created. 2) The value of a local minimum is nondecreasing, and the value of a local maximum is nonincreasing.

Therefore, the total variation of the solution is nonincreasing, or TVD, that is,

$$\mathrm{TV}(\phi^{n+1}) \le \mathrm{TV}(\phi^n) \tag{2}$$

$$\mathrm{TV}(\phi^n) = \Sigma_i \left|\Delta_{i+\frac{1}{2}}\phi^n\right| \tag{3}$$

where $\Delta_{i+1/2}\phi = \phi_{i+1} - \phi_i$.

If the numerical scheme is written in the form

$$\phi_i^{n+1} = \phi_i^n - C_{i-\frac{1}{2}}\Delta_{i-\frac{1}{2}}\phi^n + D_{i+\frac{1}{2}}\Delta_{i+\frac{1}{2}}\phi^n \tag{4}$$

where $C_{i-1/2}$ and $D_{i+1/2}$ are data-dependent coefficients, sufficient conditions for the scheme to secure the TVD inequalities are[7]

$$0 \le C_{i-\frac{1}{2}}, \qquad 0 \le D_{i+\frac{1}{2}}, \qquad 0 \le C_{i-\frac{1}{2}} + D_{i+\frac{1}{2}} \le 1 \tag{5}$$

Following Sweby's formulation,[9] the discretized form of the scalar equation can be expressed as a combination of a first-order scheme and an antidiffusive flux:

$$\phi_i^{n+1} = \phi_i^n - \underbrace{\nu\left\{1 + \frac{1}{2}(1-\nu)\left[\frac{\Psi\left(r_{i+\frac{1}{2}}\right)}{r_{i+\frac{1}{2}}} - \Psi\left(r_{i-\frac{1}{2}}\right)\right]\right\}}_{C_{i-\frac{1}{2}}}\Delta_{i-\frac{1}{2}}\phi^n \tag{6}$$

Received 28 October 1998; presented as Paper 99-3262 at the AIAA 14th Computational Fluid Dynamics Conference, Norfolk, VA, 28 June–1 July 1999; revision received 7 December 1999; accepted for publication 7 May 2000. Copyright © 2000 by K. B. Kuan and C. A. Lin. Published by the American Institute of Aeronautics and Astronautics, Inc., with permission.

*Graduate Student, Department of Power Mechanical Engineering.
†Professor, Department of Power Mechanical Engineering. Senior Member AIAA.

where Ψ is the flux limiter, which determines the level of antidiffusive flux; $\nu = a\,\delta t/\delta x$; and $r_{i+1/2} = \Delta_{i-1/2}\phi^n/\Delta_{i+1/2}\phi^n$. Note that Eq. (6) is a modified form of the Lax–Wendroff scheme, and the original Lax–Wendroff scheme is recovered by setting $\Psi = 1$.

It is apparent that the preceding formulation shows that $D_{i+1/2} = 0$. Therefore, for the scheme to satisfy the TVD constraints, the following prevails:

$$0 \le \nu\left\{1 + \frac{1}{2}(1-\nu)\left[\frac{\Psi\left(r_{i+\frac{1}{2}}\right)}{r_{i+\frac{1}{2}}} - \Psi\left(r_{i-\frac{1}{2}}\right)\right]\right\} \le 1 \tag{7}$$

It can be shown that the left inequality of Eq. (7) is satisfied when[15]

$$\Psi\left(r_{i-\frac{1}{2}}\right) \le 2/(1-\nu) \tag{8}$$

$$\frac{\Psi\left(r_{i+\frac{1}{2}}\right)}{r_{i+\frac{1}{2}}} \ge 0 \tag{9}$$

provided that $\nu < 1$.

As for the right inequality of Eq. (7), by the introduction of a parameter β (Ref. 15), it can be shown that

$$0 \le \frac{\nu}{2}(1-\nu)\frac{\Psi\left(r_{i+\frac{1}{2}}\right)}{r_{i+\frac{1}{2}}} \le \beta \tag{10}$$

$$0 \le (\nu/2)\left[2 - (1-\nu)\Psi\left(r_{i-\frac{1}{2}}\right)\right] \le 1 - \beta \tag{11}$$

Equations (10) and (11) can be rearranged to give

$$0 \le \frac{\Psi\left(r_{i+\frac{1}{2}}\right)}{r_{i+\frac{1}{2}}} \le \frac{2\beta}{\nu(1-\nu)} \tag{12}$$

$$\frac{2(\beta-1)}{\nu(1-\nu)} + \frac{2}{1-\nu} \le \Psi\left(r_{i-\frac{1}{2}}\right) \tag{13}$$

Because the lower limit of Ψ is zero, the value of β is $1-\nu$. Therefore, the unsteady TVD constraints dictate that

$$\begin{aligned} 0 < \Psi(r) &\le \min[2/(1-\nu), 2r/\nu], \quad \text{for} \quad r > 0 \\ \Psi(r) &= 0, \quad \text{for} \quad r \le 0 \end{aligned} \tag{14}$$

These represent the upper bound of the unsteady or adaptive TVD constraints, which were proposed by Jeng and Payne.[15] Other Courant-number-dependent bounding properties[12–14] were also proposed, but the results from the TVD derivation are straightforward and are adopted here.

A subset of the preceding TVD constraints was proposed by Sweby[9]

$$\begin{aligned} 0 < \Psi(r) &\le \min[2, 2r], \quad \text{for} \quad r > 0 \\ \Psi(r) &= 0, \quad \text{for} \quad r \le 0 \end{aligned} \tag{15}$$

The range of both TVD constraints can be seen from Fig. 1, where the dashed and dot–dashed lines correspond to Eqs. (14) and (15), respectively. It is clear that Sweby's[9] constraints are more restrictive than the adaptive one.

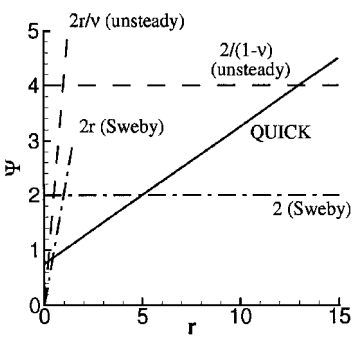

Fig. 1 TVD range.

III. Adaptive QUICK-Based Scheme

For most steady flow computations employing the pressure-based method and segregated approach, the third-order accuare QUICK[2] scheme is usually adopted. Therefore, it will be beneficial to introduce the TVD concept into the scheme.

If expressed in terms of a flux limiter, the QUICK scheme can be written as

$$\Psi(r)_{\text{QUICK}} = 0.75 + 0.25r \tag{16}$$

This line is shown in Fig. 1, and it can be clearly seen that a higher proportion of the QUICK scheme lies outside the aforementioned TVD range. Therefore, it is not surprising to observe the scheme to produce over- and undershoots in regions where the convected variables experience sharp changes in gradient or discontinuities under highly convective conditions.

To remedy this and still maintain a high order of accuracy, a bounded QUICK scheme[6] was proposed:

$$\Psi(r)_{\text{bounded-QUICK}} = \max[0, \min(2, 2r, 0.75 + 0.25r)] \tag{17}$$

This can be seen as a nonlinear functional relationship bounded by Sweby's[9] TVD constraints.

To account for the Courant number effect, as indicated by the adaptive TVD constraints, an adaptive QUICK scheme can be formulated, and the authors suggest the following new scheme:

$$\Psi(r)_{\text{adaptive-QUICK}} = \max\{0, \min[\underbrace{2/(1-\nu), 2r/\nu}_{\text{unsteady TVD}}, \underbrace{0.75 + 0.25r}_{\text{QUICK}}]\} \tag{18}$$

It can be clearly seen that the region adopting the QUICK scheme has been increased dramatically by adopting the adaptive TVD constraints. Because the regions for the proposed scheme to coincide with the QUICK scheme are more than those of the bounded-QUICK scheme, the accuracy of the present scheme might be higher. Therefore, less diffusive results might be expected.

IV. Solution Algorithm

The discretized form of the scalar equation,

$$U_t + F(U)_x = 0 \tag{19}$$

can be expressed as

$$U_i^{n+1} = U_i^n - \frac{\delta t}{\delta x}\left[\tilde{F}^n_{i+\frac{1}{2}} - \tilde{F}^n_{i-\frac{1}{2}}\right] \tag{20}$$

Following Roe[16] and Sweby,[9] the flux $\tilde{F}_{i+1/2}$ can be expressed as

$$\begin{aligned} &\frac{1}{2}[F_i + F_{i+1} - \text{sign}(a)(F_{i+1} - F_i)] \\ &\quad + \frac{1}{2}\Psi\left(r_{i+\frac{1}{2}}\right)\left[\text{sign}(a) - a\frac{\delta t}{\delta x}\right](F_{i+1} - F_i) \end{aligned} \tag{21}$$

where $a = \partial F/\partial U$ and Ψ is the flux limiter. This scheme is second-order accurate in time and space.

The discretized form of the Euler equation (in one direction for simplicity) can be expressed as

$$U_i^{n+1} = U_i^n - \nu\left[\tilde{F}^n_{i+\frac{1}{2}} - \tilde{F}^n_{i-\frac{1}{2}}\right] \tag{22}$$

where $\nu = \delta t/\delta x$ and

$$U = \begin{bmatrix} \rho \\ \rho U \\ \rho e \end{bmatrix}, \qquad F = \begin{bmatrix} \rho U \\ \rho U^2 + P \\ (\rho e + P)U \end{bmatrix}$$

Following Yee,[17] the flux $\tilde{F}$ is expressed as

$$\tilde{F}^n_{i+\frac{1}{2}} = \tfrac{1}{2}\left[F^n_i + F^n_{i+1} - R^n_{i+\frac{1}{2}}\Phi^n_{i+\frac{1}{2}}\right] \tag{23}$$

$$\frac{\partial F}{\partial U} = R\Lambda(\lambda)R^- \tag{24}$$

$$\Phi_{i+\frac{1}{2}} = \left\{\nu\beta\left(\lambda_{i+\frac{1}{2}}\right)^2\Psi\left(r_{i+\frac{1}{2}}\right) + Q\left(\lambda_{i+\frac{1}{2}}\right)\left[1-\Psi\left(r_{i+\frac{1}{2}}\right)\right]\right\}\alpha_{i+\frac{1}{2}} \tag{25}$$

$$\alpha_{j+\frac{1}{2}} = R^-_{i+\frac{1}{2}}\Delta_{i+\frac{1}{2}}U$$

$$Q(z) = \begin{cases} |z|, & \text{if} \quad |z| \le \epsilon \\ (z^2+\epsilon^2)/2\epsilon, & \text{others} \end{cases}$$

where λ is the eigenvalue and β is 0 and 1 for steady and transient solutions, respectively. This scheme is second-order accurate in space and, when $\beta = 1$, is second-order accurate in time.[17]

The determination of $r_{i+1/2}$ is given by the following expression:

$$r_{i+\frac{1}{2}} = \tfrac{1}{2}\left[\lambda_{i+\frac{1}{2}}\left(\alpha_{i-\frac{1}{2}} + \alpha_{i+\frac{3}{2}}\right) + \left|\lambda_{i+\frac{1}{2}}\right|\left(\alpha_{i-\frac{1}{2}} - \alpha_{i+\frac{3}{2}}\right)\right]\Big/\left(\lambda_{i+\frac{1}{2}}\alpha_{i+\frac{1}{2}}\right) \tag{26}$$

or

$$r_{i+\frac{1}{2}} = \tfrac{1}{2}\left[\lambda_{i+\frac{1}{2}}\left(\lambda_{i-\frac{1}{2}}\alpha_{i-\frac{1}{2}} + \lambda_{i+\frac{3}{2}}\alpha_{i+\frac{3}{2}}\right) + \left|\lambda_{i+\frac{1}{2}}\right|\left(\lambda_{i-\frac{1}{2}}\alpha_{i-\frac{1}{2}} - \lambda_{i+\frac{3}{2}}\alpha_{i+\frac{3}{2}}\right)\right]\Big/\left(\lambda^2_{i+\frac{1}{2}}\alpha_{i+\frac{1}{2}}\right) \tag{27}$$

In the present approach, the latter formulation is usually adopted.

V. Results and Discussion

A. Unsteady Linear Advection Equation

The purpose of this test is to verify the second-order accuracy of the proposed scheme. Consider a linear advection equation, and the governing equation can be written as

$$\frac{\partial U}{\partial t} + a\frac{\partial U}{\partial x} = 0.0$$

Because this is an initial value problem, the exact solution can be expressed as $U(x;t) = U_0(x-at)$, where $U_0(x)$ is the initial condition. To further simplify the solution procedure, a periodic boundary condition is imposed.

Consider, first, a simple problem with the following initial condition:

$$U_0(x) = -0.5\sin\pi x + 0.5, \qquad -1 < x < 1$$

The Courant numbers ν for the present case are 0.2, 0.5, and 0.8, respectively, and the grid points adopted are 21, 41, 81, 161, 321, and 641. The computations end at time $t = 1.0$. Figure 2 shows the variation of the L_1 and L_2 norms at different mesh sizes (dX) and Courant–Friedrichs–Lewy (CFL) numbers. The order of accuracy of the L_1 and L_2 error norms is about 2 and 1.7, respectively. This indicates that the proposed scheme is second-order accurate. Also note that the absolute error of the CFL $= 0.8$ case is the lowest, which indicates that the level of accuracy is the highest. These results are not surprising. Because the unsteady TVD region is bounded by $2/(1-\nu)$ and $2r/\nu$, therefore, the regions for the proposed scheme to coincide with the QUICK scheme for CFL $= 0.8$ is higher, as shown in Fig. 1.

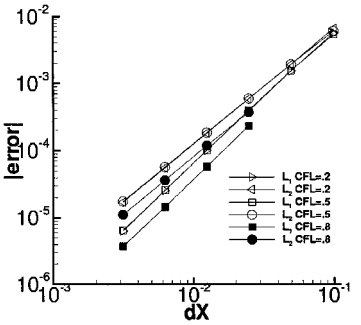

Fig. 2 Solution error of linear advection equation: smooth profile, A-Q scheme.

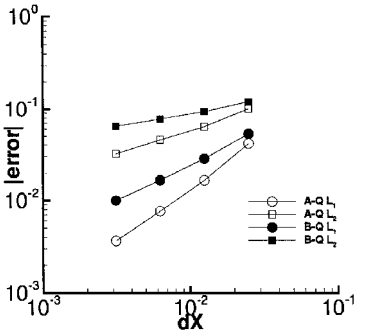

Fig. 3 Solution error of linear advection equation: rough profile, $\nu = 0.8$.

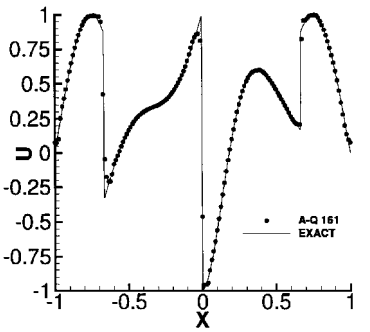

Fig. 4 Predicted results of linear advection equation: rough profile, $\nu = 0.8$.

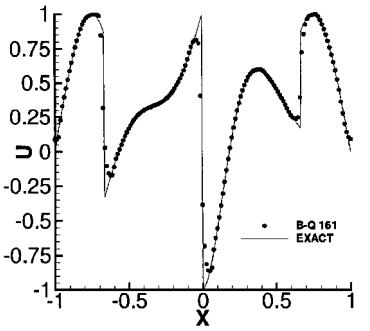

Fig. 5 Predicted results of linear advection equation: rough profile, $\nu = 0.8$.

The proposed scheme is further applied to the linear advection problem with sharp gradients of the transported properties. The case adopted here was also examined by Harten,[18] and the initial condition takes the form as

$$U_0(x) = \begin{cases} -x\sin(3\pi x^2/2), & -1 \le x \le \frac{1}{3} \\ |\sin(2\pi x)|, & |x| < \frac{1}{3} \\ 2x - 1 - [\sin(3\pi x)/6], & \frac{1}{3} < x < 1 \end{cases}$$

Computations are performed with CFL $= 0.8$ and end at time $t = 1$. The solution errors are shown in Fig. 3, and it can be seen that the adaptive-QUICK (A-Q) results are much more accurate than the bounded-QUICK (B-Q) results. The predicted results, shown in Figs. 4 and 5, confirm this. It is not surprising to observe that the B-Q is slightly more diffusive. Note that the contact discontinuity sharpening technique, similar to that adopted by Jeng and Payne,[15] is adopted here.

B. Unsteady Burgers Equation

The performance of the proposed scheme is next examined by applying to the nonlinear Burgers equation

$$\frac{\partial U}{\partial t} + \frac{\partial f}{\partial x} = 0 \tag{28}$$

where $f = U^2/2$.

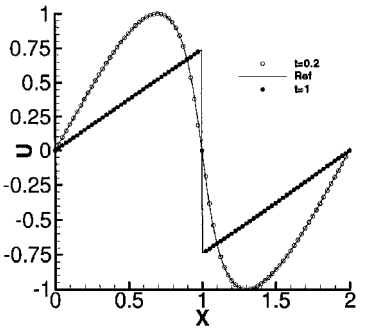

Fig. 6 Predicted results of Burgers equation: A-Q scheme, 81 points, and $\nu = 0.8$.

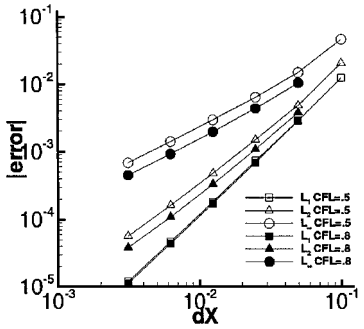

Fig. 7 Solution error of Burgers equation: $t = 1$, A-Q scheme.

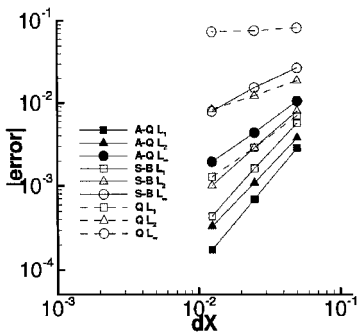

Fig. 8 Solution error of Burgers equation of different schemes: $t = 1$, $\nu = 0.8$.

This is an initial value problem and, to simplify the solution procedure, a periodic boundary condition is imposed. The initial condition is set as

$$U(x, 0) = \sin(\pi x), \qquad 0 < x < 2$$

The reference solution is the result of the numerical solution using 5001 grid points. Figure 6 shows the predicted solution at two different times, $t = 0.2$ and 1, adopting the A-Q scheme. It can be clearly observed that the formation of the shock appears at $t = 1$, and the performance of the proposed scheme in reproducing the shock is excellent. The detailed analysis of the solution error can be directed to Fig. 7, which shows the solution error at time $t = 1$ with different grid sizes and CFL numbers. At time $t = 1$, the CFL $= 0.8$ case performs the best, though the difference of the L_1 norm is marginal. Overall, the CFL $= 0.8$ is better. Therefore, in subsequent computations this CFL number will be adopted. The orders of accuracy of the present scheme are 2 and 1.7 for the L_1 and L_2 error norm. These are not affected by the presence of the shock. Figure 8 shows the comparisons of the solution error using different schemes, that is, Super-Bee (S-B), QUICK (Q), and the present scheme at $t = 1$. It can be clearly seen that the absolute error of the present scheme is the lowest. On the other hand, it is not surprising to see that the Q scheme has the highest level of error, which is due to the oscillating solution across the shock.

C. Unsteady One-Dimensional Shock Tube Problem

In contrast to the preceding scalar cases, attention is focused here on an unsteady nonlinear shock-tube problem.

The initial conditions of the problem

$$\rho = 1, \qquad P = 1, \qquad U = 0, \qquad 0 \le x < 0.5$$
$$\rho = 0.25, \qquad P = 0.1, \qquad U = 0, \qquad 0.5 < x \le 1$$

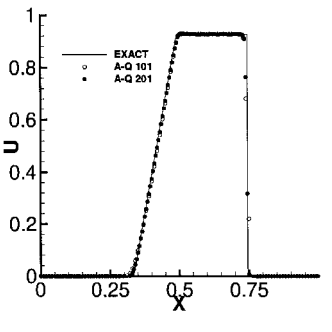

Fig. 9 Predicted velocity of shock tube problem with different grid densities: $t = 0.14$.

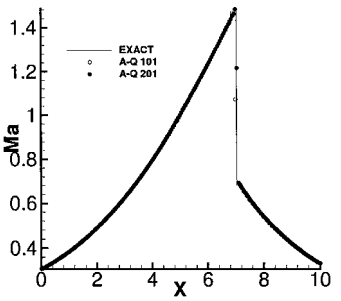

Fig. 10 Predicted Mach number distribution of Laval nozzle.

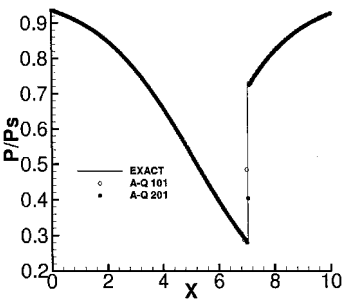

Fig. 11 Predicted pressure distribution of Laval nozzle.

consist of two stagnant regions with different densities and pressures separated by a diaphragm placed at $x = 0.5$. At time $t = 0$, the diaphragm is ruptured, and a series of compression waves rapidly coalesce into a normal shock. Simulations with $dt = 0.001$ and 140 time steps focus on the case before any wave has reached the boundaries. Figure 9 shows the predicted velocity distributions using different grid densities. The results indicate that the number of grid point across the shock remains the same, indicating the accuracy of the scheme proposed.

D. Steady One-Dimensional Laval Nozzle Flow

Although this case is also concerned with the representation of shock, a steady Laval nozzle flow is considered here. The geometry of the nozzle is

$$A(x) = A_{\text{tr}} + (A_i - A_{\text{tr}})[(5 - x)/5]^2, \qquad x \le 5$$
$$A(x) = A_{\text{tr}} + (A_e - A_{\text{tr}})[(x - 5)/5]^2, \qquad x \ge 5 \qquad (29)$$

where A_i, A_{tr}, A_e are the inlet, throat, and exit area of the nozzle with area ratio of 2:1:2; the range of the nozzle spans from 0 to 10.

Computations were performed with 101–201 uniform grid nodes. The Mach number and pressure variations along the nozzle with the $P_e/P_0 = 0.86$ exit pressure ratios are shown in Figs. 10 and 11. It can be seen that the proposed schemes show oscillation free results and high level of accuracy. The number of grid points across the shock using different grid density remains the same.

E. Steady Two-Dimensional Oblique Shock Flow

The applicability of the present method to a two-dimensional shock problem, where an inviscid flow developed by a shock wave reflects from a rigid surface, is considered. Figure 12 shows the geometry and pressure solutions for the shock reflection problem. The computational domain is a rectangle of length 4 and height 1, with a uniform grid sizes of 121 × 41 and 241 × 82. The boundary

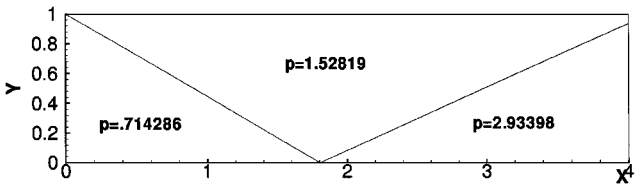

Fig. 12 Configuration of oblique shock problem.

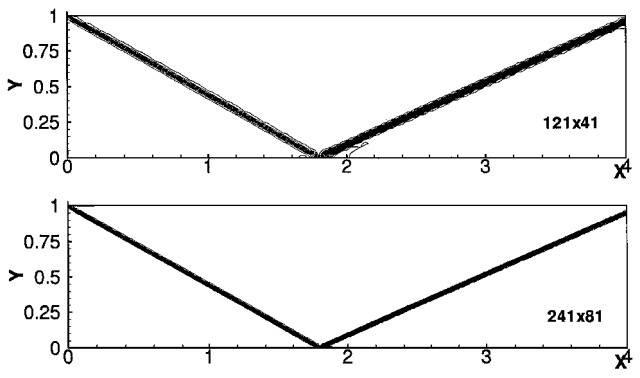

Fig. 13 Predicted pressure distribution.

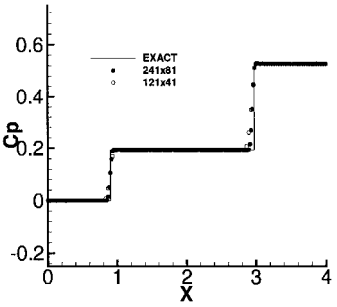

Fig. 14 Predicted pressure coefficients.

conditions are that of a reflecting surface along the bottom surface, supersonic outflow along the right surface, and prescribed fixed values on the other two sides, which are

$$(\rho, u, v, p)_{(0,y,t)} = \left(1, 2.9, 0, \tfrac{1}{1.4}\right)$$

$$(\rho, u, v, p)_{(x,1,t)} = (1.69997, 2.61934, -0.50632, 1.52819)$$

The boundary conditions produce an incident shock angle of 29 deg and the freestream Mach number M_∞ was 2.9. The numerical algorithm adopted here is the direct two-dimensional extension of the one-dimensional methods employed to calculate the shock tube problem, albeit the present case is concerned with two-dimensional steady-state solution.

Figure 13 shows the pressure contours with equal contour spacing of 0.1. Both grids generate similar results and produce sharp shock capturing capability. The pressure coefficient, $C_p = (p/p_\infty - 1)2/(\gamma M_\infty^2)$ evaluated at $Y = 0.5$, is shown in Fig. 14. The incident shock is well represented by the present scheme, though the location of the reflected shock is slightly smeared. However, the overall resolution is still reasonable.

VI. Conclusions

A new high-order-accurate convection scheme, which satisfies the unsteady TVD principle, has been developed. Numerical experiments indicate that the proposed scheme is second-order accurate when applied to linear and nonlinear scalar equations. The scheme was also shown to be able to capture the sharp gradients of the scalar profiles. The proposed scheme was further applied to one-dimensional shock tube and Laval nozzle flows, and a two-dimensional steady shock reflection problem. Predicted results for the unsteady shock-tube flow, steady Laval nozzle flow and the two-dimensional shock reflection problem indicate the present method returned accurate and oscillation free results.

Acknowledgment

This research work was supported by the National Science Council of Taiwan under Grant NSC-85-2212-E-007-057.

References

[1]Jameson, A., Schmidt, W., and Turkel, E., "Numerical Simulation of the Euler Equation by Finite Volume Methods using Runge–Kutta Time-Stepping Schemes," AIAA Paper 81-1259, 1981.

[2]Leonard, B. P., "A Stable and Accurate Convective Modelling Procedure Based on Quadratic Upstream Interpolation," *Computer Methods in Applied Mechanics and Engineering*, Vol. 19, No. 1, 1979, pp. 59–98.

[3]Leonard, B. P., "Simple High Accuracy Resolution Program for Convective Modelling of Discontinuities," *International Journal of Numerical Methods in Fluids*, Vol. 8, No. 10, 1988, pp. 1291–1318.

[4]Gaskell, P. H., and Lau, A. K. C., "Curvature-Compensated Convective Transport: SMART, A New Boundedness-Preserving Transport Algorithm," *International Journal of Numerical Methods in Fluids*, Vol. 8, No. 6, 1988, pp. 617–641.

[5]Lin, H., and Chieng, C. C., "Characteristic-Based Flux Limiter of an Essentially 3rd-Order Flux-Splitting Method for Hyperbolic Conservation Laws," *International Journal of Numerical Methods in Fluids*, Vol. 13, No. 3, 1991, pp. 287–301.

[6]Lin, C.-H., and Lin, C. A., "Simple High-Order Bounded Convection Scheme to Model Discontinuities," *AIAA Journal*, Vol. 35, No. 3, 1997, pp. 563–565.

[7]Harten, A., "High Resolution Schemes for Hyperbolic Conservation Laws," *Journal of Computational Physics*, Vol. 49, No. 3, 1983, pp. 357–393.

[8]Harten, A., "On a Class of High Resolution Total-Variation-Stable Finite-Difference Scheme," *SIAM Journal on Numerical Analysis*, Vol. 21, No. 1, 1984, pp. 1–23.

[9]Sweby, P. K., "High Resolution Schemes Using Flux Limiters for Hyperbolic Conservation Laws," *SIAM Journal on Numerical Analysis*, Vol. 21, No. 5, 1984, pp. 995–1011.

[10]Yee, H. C., Warming, R. F., and Harten, A., "Implicit Total Variation Diminishing (TVD) Schemes for Steady-State Calculations," *Journal of Computational Physics*, Vol. 57, No. 3, 1985, pp. 327–360.

[11]Lien, F. S., and Leschziner, M. A., "Upstream Monotonic Interpolation for Scalar Transport with Applications to Complex Turbulent Flows," *International Journal of Numerical Methods in Fluids*, Vol. 19, No. 6, 1994, pp. 527–548.

[12]Roe, P. L., and Baines, M. J., "Asymptotic Behaviour of Some Non-Linear Schemes for Linear Advection," *Proceedings of the 5th GAMM Conference on Numerical Methods in Fluid Mechanics*, edited by M. Pandolfi and R. Piva, Vieweg and Sohn, Braunschweig, Germany, 1983, pp. 283–290.

[13]Leonard, B. P., and Niknafs, H. S., "Sharp Monotonic Resolution of Discontinuities Without Clipping of Narrow Extrema," *Computer and Fluids*, Vol. 19, No. 1, 1991, pp. 141–154.

[14]Leonard, B. P., "The ULTIMATE Conservative Difference Scheme Applied to Unsteady One-Dimensional Advection," *Computer Methods in Applied Mechanics and Engineering*, Vol. 88, No. 1, 1991, pp. 17–74.

[15]Jeng, Y. N., and Payne, U. J., "An Adaptive TVD Limiter," *Journal of Computational Physics*, Vol. 118, No. 2, 1995, pp. 229-241.

[16]Roe, P. L., "Some Contribution to the Modelling of Discontinuous Flow," *Lectures in Applied Mathematics*, Vol. 22, American Mathematical Society, Providence, RI, 1985.

[17]Yee, H. C., "Construction of Explicit and Implicit Symmetric TVD Schemes and Their Applications," *Journal of Computational Physics*, Vol. 68, No. 1, 1987, pp. 151–179.

[18]Harten, A., "ENO Schemes with Subcell Resolution," *Journal of Computational Physics*, Vol. 83, No. 1, 1989, pp. 148–184.

G. M. Faeth
Editor-in-Chief